# Unsteady PSP Measurements of the Shock Dynamics on a Transonic Laminar Airfoil

Marie-Claire Merienne, Vincent Brion, Jean-Charles Abart

# Unsteady PSP Measurements of the Shock Dynamics on a Transonic Laminar Airfoil

M.C. Mérienne[1], V. Brion[2] and J.-C. Abart[3]
*ONERA, The French Aerospace Lab, 92190 Meudon, France*

**Unsteady Pressure Sensitive Paint is applied to measure and investigate the shock dynamics on a transonic laminar airfoil which exhibits a rapid shock oscillation at a normalized frequency, based on chord and freestream velocity, close to one. The main motivation is to assess the capability of the PSP technique to capture the pressure fluctuations imposed at the upper surface of the wing by the oscillating shock wave, in the light of the recent developments performed at ONERA of the unsteady Anodized-Aluminum PSP method. Beyond frequency resolution, it is found that three main difficulties arise when applying PSP for the present unsteady laminar flow. The first concerns the roughness of the PSP layer, which must remain low to prevent unwanted transition of the laminar boundary layer. The second deals with the correction of illumination as compressibility and wing deformations may affect it. The third is about the correction of the temperature sensitivity of the PSP, which is mandatory in the present high speed flow situation. These three questions are carefully addressed. In addition, measurements for the case when the boundary layer at the upper surface of the airfoil is made fully turbulent by forced tripping are carried out for reference. In this case the dynamics is much slower, with a normalized frequency close to 0.05. The PSP pressure fields offer a rich database to analyze the flow features. In particular the spatial sampling provided by the PSP helps to qualify the two-dimensional nature of the shock movements and to question the wave propagation process implied by these unsteadiness.**

## I. Introduction

Shock Buffet acts as a limiting factor in the working speed and incidence of transonic wings. This phenomenon corresponds to the oscillations, above some critical aerodynamic loading, of the shock system that naturally forms at the wing surface in transonic conditions. The unsteady loads that result can generate a dangerous excitation to the structure of the wing. In the design phase of an aircraft, margins to buffet are considered which are based on estimated buffet threshold. Even today buffet predictions remain plagued by large uncertainties. This acts negatively on the efficiency of the wing design that can be achieved.

Buffet is particularly harmful for two-dimensional configurations, i.e. airfoils, as the shock may oscillate over a significant portion of the chord at a well-defined, rather low, frequency [**1**], [**2**]. This is in sharp comparison with buffet on three-dimensional wings which appears on a broad range of low frequency spectrum [**3**]. While these results were obtained for wing in fully turbulent flow, the existence and nature of buffet for laminar wings has been questioned recently, as it did not seem to have ever been described, except for the analysis of Dor et al. [**4**], which however left the subject still mostly open. There is currently a renewed interest for extended laminar flow regions on aerodynamic bodies to reduce drag. The Buterfli project co-funded by Europe and Russia was dedicated to investigate laminar buffet dynamics by setting up an experiment using a laminar airfoil. The analysis of Brion et al. [**5**] based on these tests shows that a laminar buffet phenomenon exists, in similarity with the fully turbulent configuration, however with a shock oscillation at a Strouhal number on the order of unity in the range of Mach numbers from 0.72 to 0.77 and incidence from 1.5 to 4 degrees, to be compared with a Strouhal number on the order of 0.01 for the turbulent flow.

In this paper, the Pressure Sensitive Paint (PSP) technique is applied to measure the shock dynamics of the laminar airfoil used in the Buterfli program. The aim is two-fold. First since the frequency of the laminar buffet phenomenon is rather high (about 1000Hz for the tests to be described), it represents a challenge in terms of response time and amplitude of the PSP signal. As a comparison, the turbulent phenomenon earlier described in Jacquin et al. [**2**] which yields a Strouhal number of 0.05 corresponds to a frequency of less than 100Hz. Second,

[1] Research engineer, Department of Aerodynamics, Aeroelasticity and Acoustics
[2] Research engineer, Department of Aerodynamics, Aeroelasticity and Acoustics
[3] Wind tunnel engineer, Department of Aerodynamics, Aeroelasticity and Acoustics

given the success of the PSP measurements, the spatial sampling provided by the PSP will serve as a valuable tool to investigate the dynamics of the flow based on its pressure signature at the airfoil surface.

Another interest in the laminar flow situation lies in the severe constraints imposed in terms of surface roughness. Basically, the average roughness size must be on the order of tenths of microns at most, that is the typical displacement thickness of the boundary layer at the upper surface of the airfoil downstream of the leading edge in laminar flow. This constraint implies that the PSP coating needs to be adequate and applied with great care. All the relevant experimental details are discussed in this paper, along with the description of the ONERA made unsteady PSP that is used. In the experimental approach the turbulent buffet phenomenon is taken as a reference. The shock frequency in this case is well within the usual temporal resolution acceptable by unsteady PSP and the shock motion exhibits a back and forth movement along the chord that can be tracked easily to validate the implementation of the PSP technique.

The paper is organized as follows. The experimental setup is first presented, including a detailed description of the PSP setup. The PSP measurements are then discussed, an analysis of the main flow features is given and comparisons with conventional pressure sensors results are presented.

## II. Experimental setup

### A. Wind tunnel setup

The test setup that is used here was initially developed by Jacquin et al. [**2**] to investigate buffet for a fully turbulent flow. The experimental setup is an airfoil installed horizontally in the test section of the S3Ch transonic wind tunnel at the ONERA Meudon research center (Figure 1). The chord of the airfoil is $c = 230mm$. The test section of the wind tunnel is L = 2.2m long, H = 0.763m in height and W = 0.804m in width. The side walls of the test section around the airfoil comprise large glass windows. The upper and lower walls are adaptive walls whose geometry is tuned axially to minimize wall interferences. The Mach number in the test section can be varied from 0.3 to 1.2 and is varied in the transonic regime for the present tests. Stagnation pressure in the settling chamber is equalized to atmospheric conditions ahead of the last turbulence mesh. Automatic temperature control maintains a uniform and constant stagnation temperature. As a result the typical Reynolds number based on chord $c$ and freestream speed $U_0$ for the tests is about $Re_c \simeq 3.10^6$.

**Figure 1. Picture of the model installed in the test section as viewed from upstream (leading edge facing). The yellow part is the PSP insert.**

The airfoil features a laminar OALT25 profile (Figure 2) which is an ONERA supercritical design that promotes extended negative pressure gradient at the upper surface of the airfoil to prevent early boundary layer transition. The flow past the airfoil was considered in two situations. First a reference configuration with the boundary layer fully turbulent (forced transition) and second the laminar configuration with the boundary layer let to evolve naturally along the upper surface (natural transition), while the lower surface is systematically forced turbulent. Boundary layer tripping is accomplished using saw-tooth tape of 0.1mm thickness and 6mm wide, the upstream edge of which is set at 7% of chord. Figure 1 shows the wing equipped with this device.

The angle of attack of the airfoil is set to 4°. The Mach number is set at two selected values, 0.72 and 0.735, that correspond to conditions above the buffet threshold in the laminar situation, and to condition below and above the buffet threshold in the turbulent situation.

The airfoil is equipped with an aluminum insert dedicated to the PSP measurements, the rest of the wing being in steel which has been polished for improved surface roughness. The chord-wise extent of the insert, as shown in Fig. 2, corresponds to $x \in [0.21; 0.78]$ in chord units. The spanwise extent is best seen in Figure 1 and corresponds to $|y| < 0.32$ in chord units, $y = 0$ being at mid-span. The insert has been set with two pressure taps and two pressure sensors to be used as references for the PSP data for the steady and unsteady part, respectively. The sensors are absolute XCQ093 models from Kulite with a range of 15 PSI. The trailing edge region of the airfoil is equipped with several pressure sensors. Absolute XCQ093 sensors with 15PSI range are used for the parts of the airfoil with sufficient thickness (square markers in Figure 2) and differential LQ062 sensors with 5PSI range are used nearest to the trailing edge (circle markers in Figure 2).

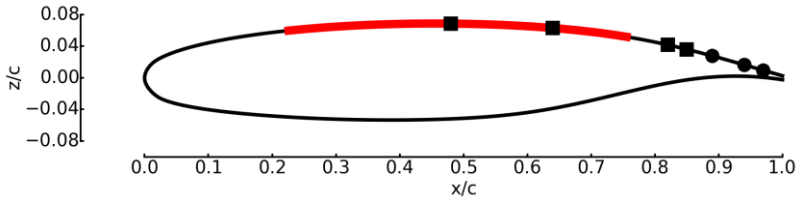


**Figure 2. Geometry of the OALT25 airfoil used for the tests. The PSP insert corresponds to the thick red line at the upper surface. The squares and circles show the locations of the pressure sensors present at the upper surface, two being in the PSP insert.**

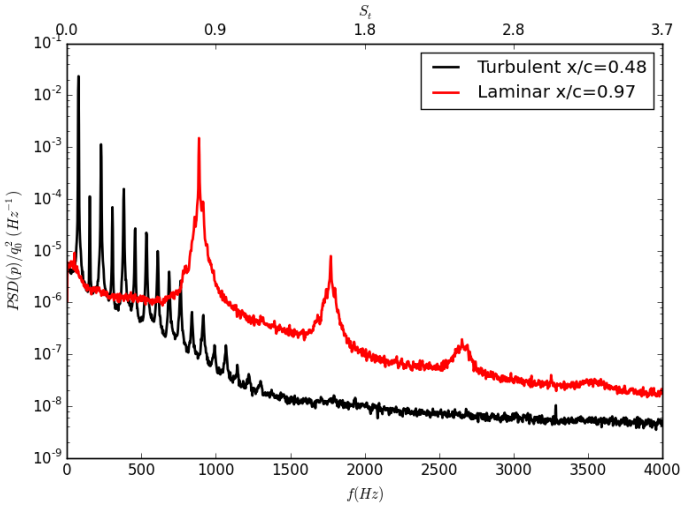


**Figure 3. Power Spectral Density of pressure fluctuations measured by the Kulite sensors located at x/c=0.48 (turbulent) and x/c=0.97 (laminar) for $M = 0.735$ and angle of attack 4°. These data were obtained in a previous test campaign, using the same model without the PSP insert and no paint. The bottom axis shows the frequency in linear scale and the top axis the corresponding Strouhal number. Comparison between the turbulent and the laminar dynamics. PSD values are normalized on freestream dynamic pressure $q_0$.**

As shown by Brion et al. [**5**], the turbulent and laminar flow configurations feature, when reaching critical angle of attack and Mach number, an unsteady shock behavior at well-marked frequencies. The corresponding Strouhal number $S_t$ is on the order of 0.05 for the turbulent case and about 1 in the laminar case. Pressure signals obtained in the region of the trailing edge using the pressure sensors capture this unsteady dynamics. The results are shown in Figure 3 in terms of normalized power spectral density (PSD) of pressure (normalized with $q_0 = \frac{1}{2}\rho U_0^2$ the dynamic pressure) as a function of frequency and Strouhal number. The pressure signals were measured in a previous experiment using the same wing but no PSP insert, using a sampling frequency of 10240Hz with duration of 40s. PSD are estimated using Welch method, with blocks of 4096 data points and 50% overlap. The PSD shape agrees

with the result obtained by Jacquin et al. [**2**] in the fully turbulent configuration. In the laminar mode the flow exhibits an unsteadiness at a much larger frequency, $S_t \simeq 0.85$. Brion et al. [**5**] describe the associated shock motion, which comprises fluctuation of the orientation of the shock foot.

The critical condition for the laminar case lies slightly below $M = 0.72$ thus the two selected Mach numbers are unsteady. In the turbulent regime the unsteadiness develops for larger angle of attack. The mach number $M = 0.72$ is a steady configuration while $M = 0.735$ is unsteady. The frequencies in physical units that correspond to the peaks identified in Figure 3 are about $80Hz$ and $1100Hz$ in the turbulent and laminar case, respectively. Two to three harmonics are also present.

### B. Unsteady PSP technique

PSP is widely used in wind tunnel testing as a mean to measure pressure at a model surface. Compared to classical pressure measurement techniques (sensors, taps), it gives a dense and wide spatial sampling. The principle of PSP is based on the oxygen quenching process of luminescent molecules. Pressure sensitive paint is a coating with such molecules embedded in it. With the air flowing past the airfoil, partial pressure of oxygen changes, which entrains a different concentration of the oxygen molecules trapped in the paint. As a consequence different external pressure levels will lead to variations in the intensity of luminescence. The luminescence process is also affected by temperature and this represents the major source of uncertainty of the PSP measurements. This point is discussed further in the text.

When dealing with unsteady PSP, the response time plays a decisive role. This factor is mostly driven by the diffusion process of oxygen molecules into the paint layer. Here a fast-responding coating is obtained by a porous structure with an open surface to speed up the diffusion process [**6**]. The binder is removed and the luminescent component is fixed directly at the model surface. The technique is originated from Asai *et al* [**7**] and Sakaue *et al.* [**8**] who have developed a fast-responding PSP based on porous anodized aluminum (AA-PSP) with the dye adsorbed on the surface. The response time of this type of coating is on the order of few tenths of microseconds.

One limitation of this technique arises from the material (aluminum) which is in general not suitable for wind tunnel test at high speeds due to the intensity of aerodynamics loads and unavoidable model deformations. The usual situation is steel made models, in which case the implementation is based on an aluminum-alloy insert that receives the PSP coating after anodization. The parameters of the paint that must be taken into account for unsteady measurements are response time, brightness and pressure/temperature sensitivities. However as it comes to laminar flow conditions the list must be supplemented with surface roughness which is, when dealing with paint, a difficult parameter to control.

Another issue is related to the illumination changes at the PSP surface due to model displacement between the reference image (without flow) and the run images under aerodynamic loads. For standard steady PSP, this correction is managed by adding a second luminescent compound which is not sensitive to pressure. This type of PSP is called binary paint. In the present case, AA-PSP does not contain such reference compound and the illumination problem arises, as is shortly discussed in section III C.

#### *1. Details of the PSP application*

The anodized aluminum PSP consists of a porous alumina layer with a self-ordered structure of micropores that are created through an electrochemical process. Figure 4 presents the different steps of this procedure. At first, the back of the insert is covered with masking latex to prevent anodization on this surface (Figure 4a). An insulated plate of PTFE (Polytetrafluoroethylene) and a shaft are then fixed to the insert. The first one is used to hold the insert and the second one allows the electrical connection during anodization (Figure 4b). The bath is a sulfuric acid solution (10 wt%) cooled at 5°C. Anodization is operated at a constant current density (15mA/cm$^2$) for 30 minutes (Figure 4c). At the end, the thickness of the porous alumina layer is about 10µm with a pore diameter of 20nm. The luminophore is then adsorbed at the surface by dipping in a solution of ruthenium complex (tris(4,7-diphenylphenanthroline) Ruthenium(II) dichloride, $[Ru(dpp)_3]Cl_2$) dissolved in dichloromethane during three minutes.

Additionally, a hydrophobic treatment is applied onto the surface because the AA-PSP coating is sensitive to humidity due to its hydrophilic nature [**9**]. One way to prevent the water adsorption is to create a hydrophobic layer on the PSP surface. This is done after the dye adsorption by dipping in a second solution of myristic acid dissolved in hexadecane with 5mM. This last stage occurs during twenty hours (Figure 4d). However, the hydrophobic treatment changes the PSP features. It increases both the luminescent signal emitted by the paint and the response time. In order to recover stable AA-PSP characteristics, the model is placed under vacuum until complete drying of the hydrophobic layer [**10**].

Once the AA-PSP coating is ready, the insert is calibrated using a pressurized chamber. The insert is then equipped with the pressure sensing devices and eventually installed in the model. The pressure sensitivity is 0.53%/kPa and the temperature sensitivity 0.8%/K. As a result, the uncertainty in pressure due to temperature is 1500Pa/K. In section II B 5, a method to correct for this effect is introduced.

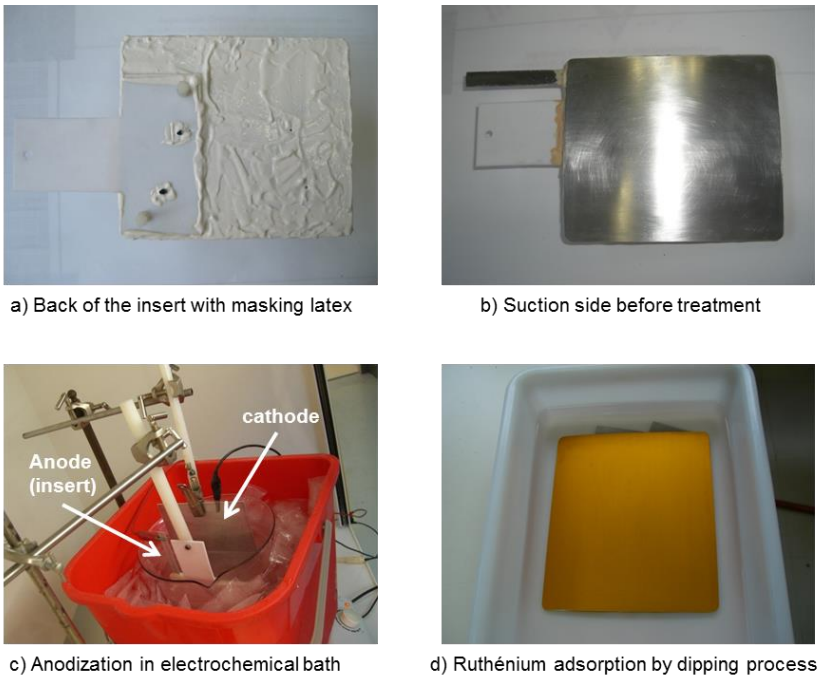


**Figure 4. Preparation of the PSP insert. Step (a) corresponds to the preparation of the insert with masking of the back side. (b) shows the upper surface to be anodized (in (c)). (d) shows the anodized insert after dipping in the Ruthenium solution.**

**Table 1. Surface roughness at the different stages of the PSP application process, compared to the raw wing made of steel.**

| Model material | Article | Ra (µm) | Rz (µm) |
|---|---|---|---|
| Steel | Clean model [**5**] | 0.3 | 2.0 |
| Al-Mg | Clean insert | 0.1 | 0.8 |
| AA-PSP | Insert with alumina layer | 0.3 | 3.3 |
| Al-Mg | Insert after removing alumina layer | 0.2 | 1.9 |

*2. Surface roughness of the painted area*

The surface roughness of the paint is an important parameter in the present study because the laminar flow conditions can be achieved only if the model surface is very smooth. Sugioka and al. [**11**] reported about the effect of PSP roughness on aerodynamic forces. They noted that increased surface roughness resulted in thicker boundary layers and enlarged separated flow areas. This generated an upstream shock location.

In the present setup, measurements with Kulite sensors obtained in a previous test campaign under the same flow conditions yielded laminar buffet frequencies at 1130Hz, that is $S_t = 1.1$ [**5**]. These were obtained with the model painted with black paint to improve infrared thermography (used in this previous work to check the transition of the boundary layer). However in a more recent work [**12**] measurements of the same laminar buffet dynamics was achieved with the same model without paint. In this case the frequency shifts to about 880Hz that is $S_t = 0.85$, as shown in Figure 3. The surface roughness without and with paint was $Ra = 0.3\mu m$ and $1.5\mu m$ respectively.

In the light of these previous findings surface roughness measurements have been performed on the PSP insert before and after coating preparation. These values are given in Table 1 and compared with the roughness of the

uncoated, steel part of the model mentioned above [**5**]. The mean surface roughness, Ra, and the peak-to-peak surface roughness, Rz, are considered. It appears that the anodization process does not change the surface roughness compared to the clean model. This represents a major advantage of the AA-PSP compared to other paints, like polymer/ceramic, used for unsteady pressure measurements [**11**].

*3. Instrumentation setup of the test section*

Instrumentation is arranged outside the wind tunnel test section looking through the lateral windows (Figure 5). AA-PSP excitation is provided with two blue LEDs at 460nm (IL-106, HardSoft) in continuous mode. They are located at both sides of the test section. A fast frame rate 12 bits CMOS camera (V710, Phantom) is used for image acquisition. In order to correct for the high angle of observation, a Scheimpflug optics, with a 105mm lens and a high pass filter (>600nm), is mounted in front of the camera. An angle of 20° for the Scheimpflug optics allows to reduce significantly image blurring (Figure 5a). The final spatial resolution is 0.15mm/pixel.

Additionally, markers are drawn at the insert surface to provide a point of view recognition and to allow image data processing according the 3D mesh of the model surface. The position of the insert, as well as pressure taps and Kulite sensors, are presented in Figure 5b.

The image acquisition rate of the camera depends on the flow conditions. In turbulent mode where the typical buffet frequency is around 80Hz, images are acquired at 1000Hz. In laminar mode, where buffet frequency lies around 1000Hz , the camera rate is set at 5000Hz. Higher acquisition rate was not possible due to the decrease of exposure time leading to lower signal-to-noise ratio. Films of 10808 images are acquired for each configuration. A reduced film of 1000 images is acquired for the reference images taken without flow.

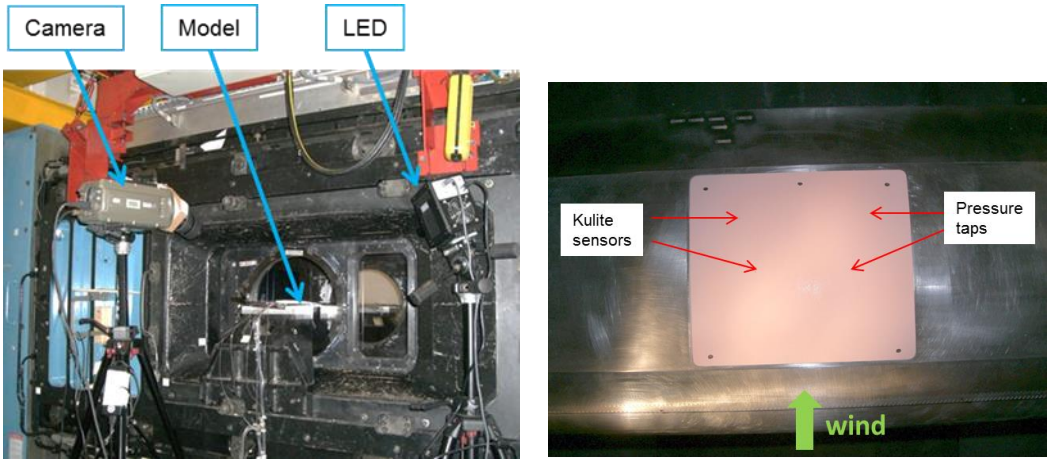


a) b)

**Figure 5. Setup in the wind tunnel. (a) Instrumentation, (b) Insert equipment on the model**

*4. Data treatment of PSP measurements*

Two sets of images are needed to process the data: *reference* images taken without flow, and *run* images taken with the flow. The ratio between these two sets of images provides the pressure field on the model surface. However this ratio cannot be computed directly because of the aerodynamic loads move and deform the model. A preliminary step is to align the two sets of images, then to compute the ratio and apply the calibration law. The main part of the data processing is this resection operation. This preprocessing is done with an in-house software developed for optical methods [**13**]. New tools have been included for unsteady applications like phase averaging, spectral analysis and cross correlation. The latest development is the implementation of the software on GPU (Graphic Processor Unit) using the CUDA language from NVIDIA. This enables to manage a large amount of images (several thousands) and to reduce dramatically the computing time by at least two orders of magnitude [**14**].

*5. Temperature correction*

One of the main corrections to be applied to PSP measurements is from temperature. As seen previously, the temperature sensitivity of the paint introduces an uncertainty of 1500Pa/K. Data processing requires the calculation of the ratio between a reference image at wind-off conditions and a run image at wind-on conditions, assuming that

the two images are recorded for the same temperature. This is not the case in general, since during a test, temperature is not uniform over the chord due primarily to differential flow speed and boundary layer state but also due to heat transfer with the material of the model.

In order to minimize this temperature effect, a reference image recorded just after the wind tunnel is switched off is used to process the PSP images. This way, the temperature difference between the two set of images (wind-off and wind-on) is reduced. Moreover, an additional correction is applied on the PSP results by using the two pressure taps implemented in the insert (see section III A).

## III. RESULTS

### A. Mean surface pressure

Figure 6 presents mean pressure distribution at the surface of the PSP insert obtained from an average of 1000 images for the turbulent and laminar cases. No spatial averaging is applied on the results. A scratch accidentally created during model handling is visible on the PSP surface. The effect of acquisition frequency, 1000Hz in the turbulent case and 5000Hz in the laminar case, leads to a significant difference on the signal-to-noise ratio. Smoother images are obtained for the acquisition rate 1000Hz that benefit from a longer exposure time. At the lowest Mach number (M=0.72), the shock locates at a position that depends on flow conditions (Figure 6a-b). In the turbulent case the shock lies at 49% of chord, while in transition free case, the shock lies at approximately 58% of chord.

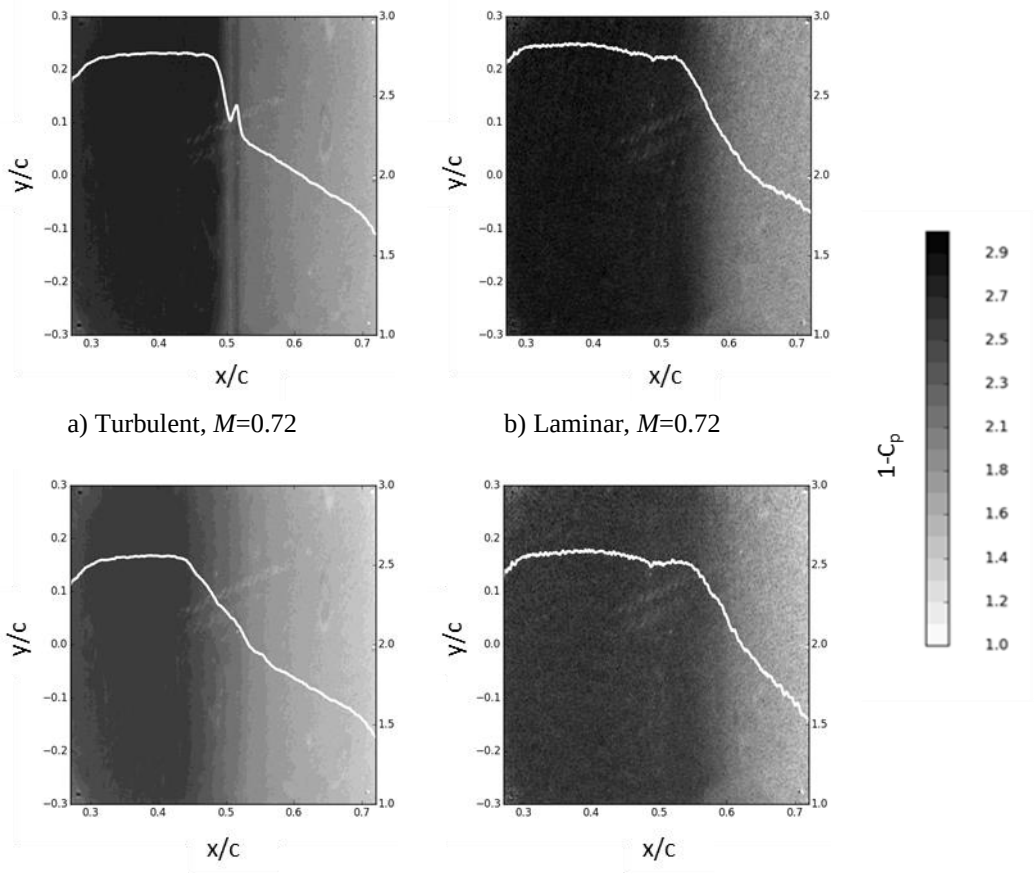


a) Turbulent, *M*=0.72 b) Laminar, *M*=0.72

c) Turbulent, *M*=0.735 d) Laminar, *M*=0.735

**Figure 6. Mean pressure distribution in terms of 1-Cp values at the surface of the PSP insert. (a) Turbulent mode M=0.72, (b) Laminar mode M=0.72, (c) Turbulent mode M=0.735, (d) Laminar mode M=0.735. Flow direction is from left to right.**

Pressure distributions as a function of chord are presented in Figure 7 for the (a-c) turbulent and (b-d) laminar cases. PSP data, smoothed over 5x5 pixels, are extracted along a chord located in the area where the two pressure taps are implemented (these pressure taps are indicated by the large dots in Figure 7). A global shift of the PSP data is applied to match the values provided by these pressure taps. The values of this shift are provided in Table 2. The shift is quite high for Mach equal to 0.72 (4 and 5kPa) but a lot smaller for Mach equal to 0.735 (400 and 600Pa).

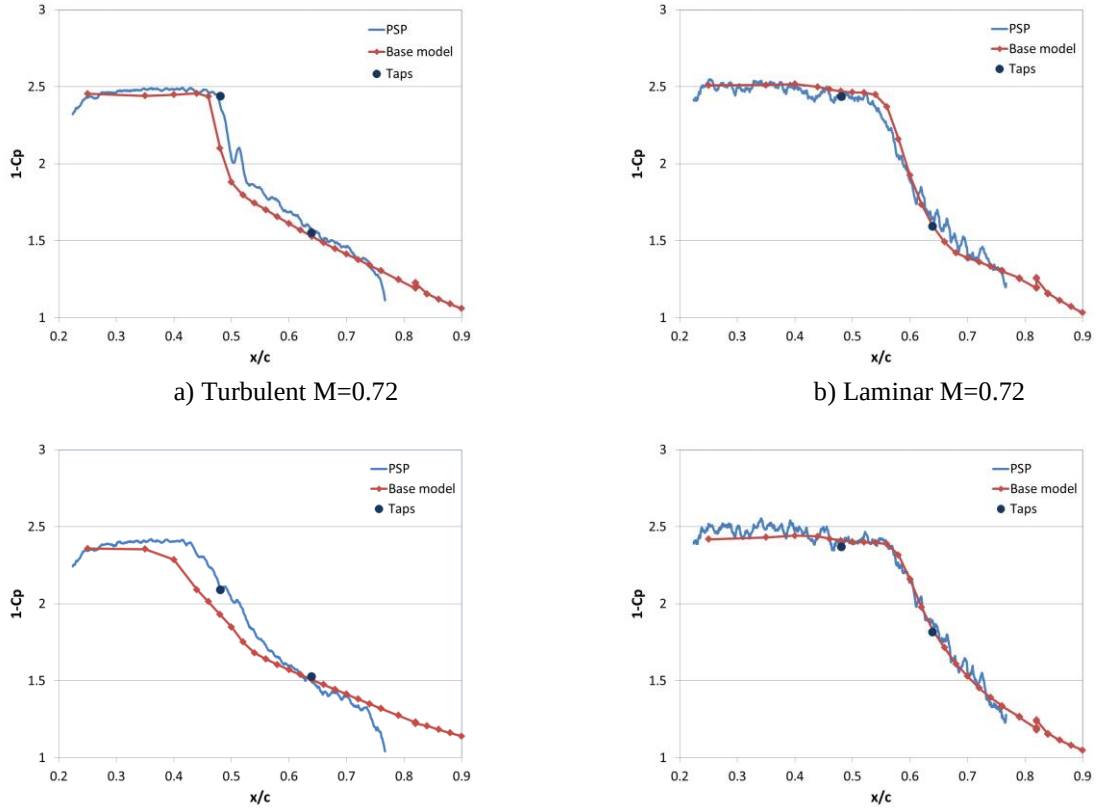


a) Turbulent M=0.72 b) Laminar M=0.72

c) Turbulent M=0.735 d) Laminar M=0.735

**Figure 7. Pressure distribution along the chord in terms of $1 - C_p$ values. Comparison of extracted PSP data and pressure tap measurements obtained on the *base model*. Large dots correspond to the pressure taps implemented in the PSP insert.**

**Table 2. Global correction applied to PSP data to match the time average pressure values given by the pressure taps.**

| Configuration | Mach Number | Shift value (Pa) | Shift value (Cp) |
|---|---|---|---|
| Turbulent | 0.72 | 4300 | 0.16 |
| | 0.735 | 600 | 0.02 |
| Laminar | 0.72 | 5300 | 0.21 |
| | 0.735 | 400 | 0.02 |

Additionally, the Cp results obtained in a previous test campaign on the model without paint (hereafter referred as *base model*) are also plotted in Figure 7. In the turbulent case, discrepancies between the *base model* and that equipped with the PSP insert are observed, mainly for Mach equal to 0.735 (Figure 7c). In general, the pressure level is constant ahead of the shock, as a result of the plateau that characterizes the airfoil geometry at the upper surface. Here, at the upstream edge of the PSP insert (x/c=0.2), an increase in pressure is present which seems doubtful since no particular variation of the airfoil geometry or external flow phenomenon can explain it. Instead we attribute this

variation to a slight misalignment between the insert and the model itself. This effect is also present for the laminar case, although with a much lower intensity. For the rest of the Cp distribution the laminar case exhibits a good agreement between the *base model* and that with the PSP insert.

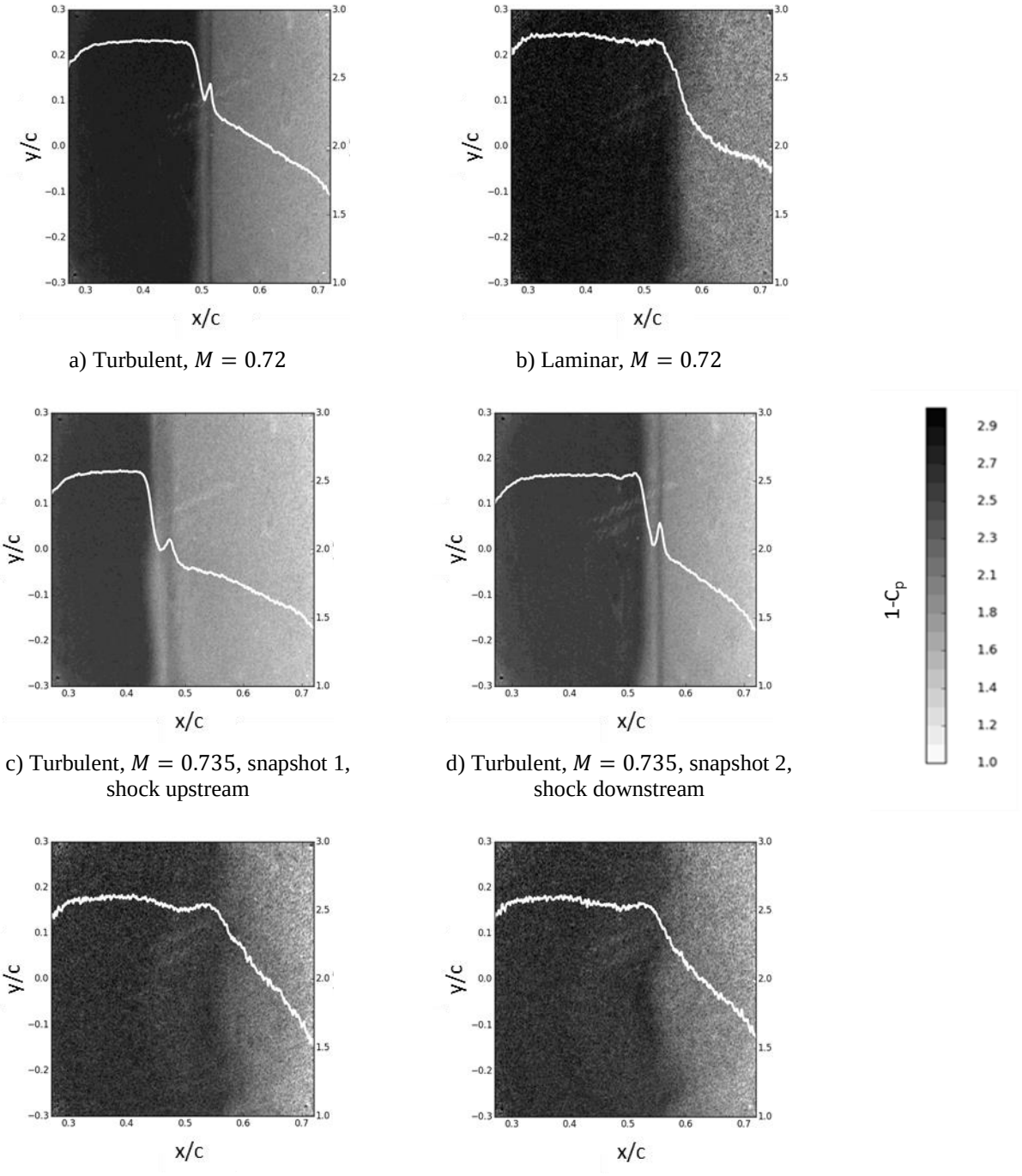


a) Turbulent, $M = 0.72$

b) Laminar, $M = 0.72$

c) Turbulent, $M = 0.735$, snapshot 1, shock upstream

d) Turbulent, $M = 0.735$, snapshot 2, shock downstream

e) Laminar, $M = 0.735$, snapshot 1

f) Laminar, $M = 0.735$, snapshot 2

**Figure 8. Snapshots of the pressure field obtained by the PSP measurements in terms of $1 - C_p$ values, for the turbulent and laminar cases at the two Mach number under investigation. The curves show the span wise average pressure along the chord wise. Flow direction is from left to right.**

### B. Instantaneous pressure

Figure 8 shows PSP snapshots for the four cases of the parametric study [turbulent, laminar]×[M=0.72, M=0.735]. For Mach 0.72 the shock is steady in the turbulent case and unsteady in the laminar case (Figure 8). For Mach 0.735 the turbulent and laminar cases are unsteady. In the latter case two snapshots are used to illustrate the effect of the shock unsteadiness on the pressure distribution.

The turbulent case in Figure 8c-d features the shock in the most upstream and downstream positions, respectively. Upstream position lies at about 44% of chord, and the downstream position lies at about 53% of chord, making a global shock displacement of approximately 9% of chord. The bump of pressure which is visible downstream of the first shock in the turbulent case is attributed to a second, weaker shock. In the laminar case for Mach equal to 0.735 and unlike the turbulent case (Figure 8e-f) the shock remains at its time average position. However the shock foot print at the wall changes significantly, indicating an oscillation of the foot of the shock wave.

### C. Spectral analysis

The PSP spectral content is first compared to the unsteady pressure measurements obtained by Kulite sensors in the previous test campaign mentioned before, with the unpainted model. Pressure kulite sensors specifically installed in the PSP insert broke down during the tests and could not be used.

For each configuration of the PSP campaign, time series of 10808 images are recorded. Power Spectral Densities (PSD) using Welch method is applied. For the PSP, blocks of 1024 images, with overlap of 50% and averaging over 20 blocks is achieved. For the Kulite measurements, as presented earlier, sampling frequency is 10240Hz, and spectral analysis is applied with blocks of 4096 samples and 50% overlap.

Figure 9 presents the data extracted in one point of the PSD images in the region of the shock wave for M=0.735, in the turbulent and laminar cases. A good agreement is found between the PSP and Kulite measurements, hence validating the PSP approach. The turbulent case exhibits the buffet frequency at 72Hz with some harmonics while in the laminar flow the fluctuations occur at 889Hz, i.e. a Strouhal number of about 0.85. Due to the increase in the noise level at high frequency, the first harmonics with low energy is weakly distinguished at 1763Hz.

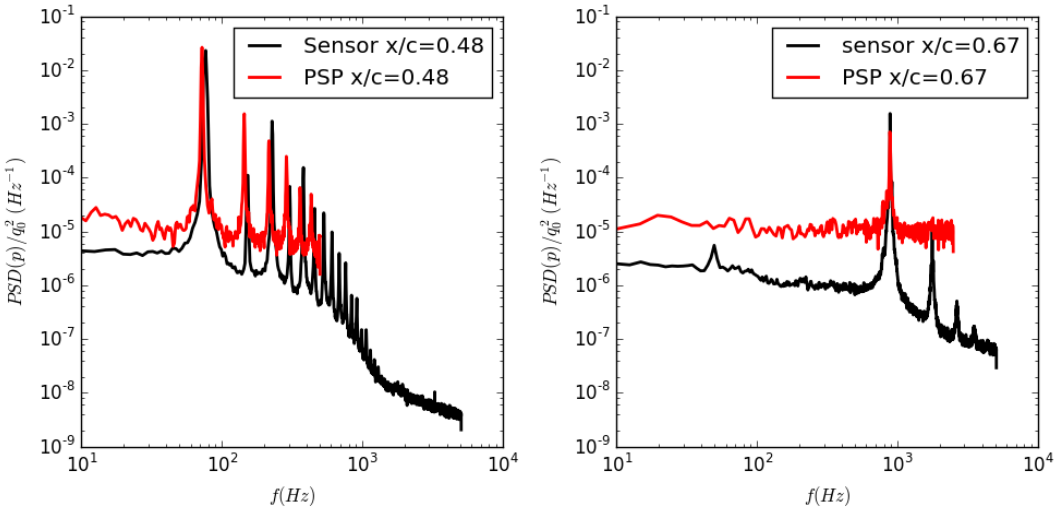


**Figure 9. Power Spectral Density of pressure at (left) x/c=0.48 for the turbulent case and (right) x/c=0.67 for the laminar case, the Mach number being set to 0.735. Comparison between PSP and Kulite measurements.**

The difference in the amplitude of the pressure fluctuation between the PSP and the sensors observed in Figure 9 is not completely explained at the moment. Three threads of interpretation are considered (i) the effect of the wing vibration that modifies the illumination field for the PSP, (ii) the unsteady flow field that generates time varying refractive index which also affects the illumination and the signal emitted by the PSP and (iii) the small gap present at the leading edge of the PSP insert that would generate increased fluctuations over a broad band of frequencies. These effects combined suggest a larger noise in the PSP data compared to data obtained from Kulite sensors as

appears from the comparison in Figure 9. To investigate the first effect, we carried out a spectral analysis of the displacement of the model that was originally used to resection the PSP images with the reference image. We found unsteady motion at very low frequency below buffet (at 13 and 23Hz) and at buffet (72Hz) in turbulent case, while in laminar case, two peaks are present at 29 and 83Hz. Concerning the second effect associated to the change in refractive index, a specific investigation would be necessary to quantify the resulting bias on the results. However, a correction of local illumination changes due to model movement, by using a second compound in the paint as mentioned in section II B, is not possible with the AA-PSP used in the present experiment.

Next the spatial distributions of the Power Spectral Density of the pressure fluctuations obtained from the PSP measurements are considered. The turbulent and laminar cases at Mach equal to 0.735 are shown in Figure 10. The dominant mode in the turbulent case (Figure 10a) indicates that most of the fluctuations are induced by the oscillations of the shock wave about its average position at about 49% of chord, the extent of oscillations being approximately 9% of chord, as noted earlier. Fluctuations downstream of the shock correspond to flow separation. The clear presence of two subharmonics in the data is reminiscent of a strong phenomenon with slight variation of the period (Figure 10b-c).

In the laminar case, a low frequency mode also protrudes in the PSD that is characterized by a slightly lower frequency than the turbulent case (Figure 10d). This suggests that the laminar flow also exhibits low frequency oscillations of the shock wave, similarly to the turbulent case but with much weaker intensity. The higher frequency modes of the laminar case, shown in Figure 10e-f with the presence of the dominant and first subharmonic modes, describe a structure significantly different from the turbulent case. First of all the mode is not 2D which can attributed to a lack of two dimensionality of the flow configuration due to the presence of the PSP insert and its lateral edges that do no perfectly align with the rest of the model. In addition the laminar mode features a larger chord-wise extent compared to the turbulent mode, with an upstream front about 20% of chord ahead of the shock wave and an intense pattern all the way down the trailing edge.

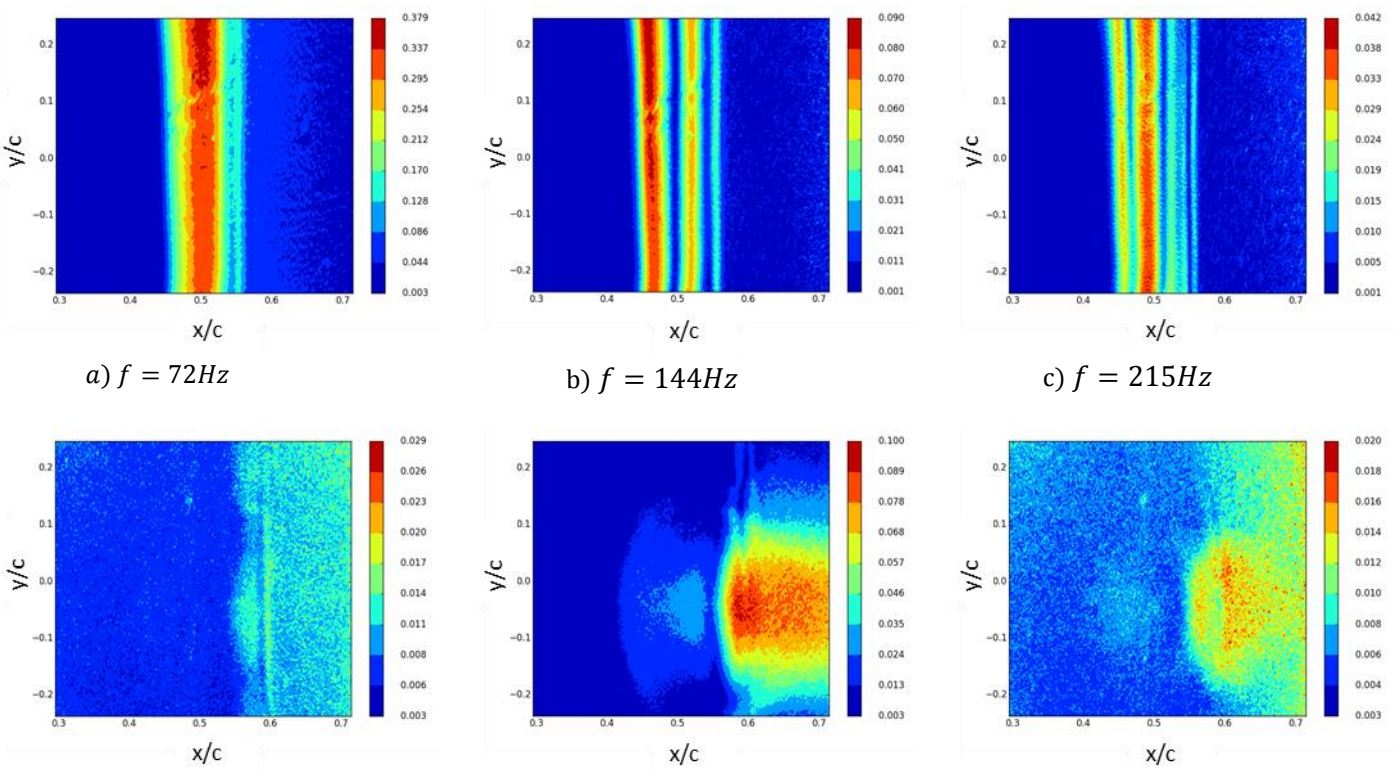


**Figure 10. Spatial distribution of the Power Spectral Density of the pressure fluctuations in terms of $-C_p$ values for (a-c) the turbulent and (d-f) laminar cases for M=0.735 for the main and subharmonic modes.**

Span-wise fluctuations of the flow field can also be observed in the PSP measurements for the turbulent case. This must be related to similar observations made by Jacquin et al. [**2**] of some span-wise deformations of the shock wave. In this respect Figure 11 shows the Power Spectral Density of the PSP data at f=38Hz, that is below the turbulent buffet frequency. Periodic oscillations of the shock wave with a span-wise wavelength of approximately $\lambda_y \sim 0.4c$ are apparent which traduce such deformation of the shock wave in span, possibly underlined by a propagating phenomenon. Similar observations have been made for other frequencies.

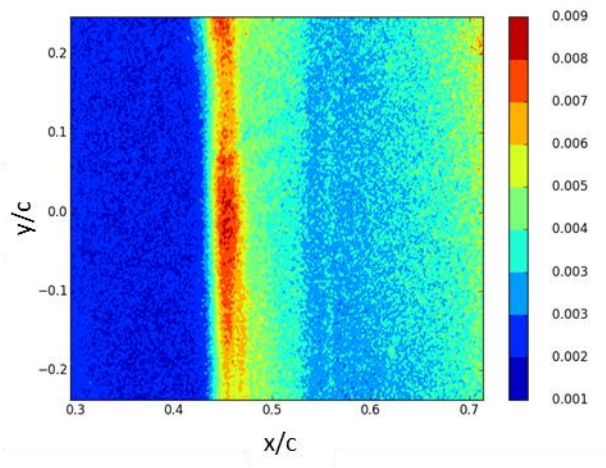


**Figure 11. Power Spectral Density of the turbulent flow, in terms of $-C_p$, for M=0.735 and f=38Hz**

The unsteadiness of the shock wave in the turbulent and laminar cases generates global oscillations of the flow field that are underpinned by propagation of disturbances. The geometry being two dimensional, information transfers mostly chord-wise although, as noticed above, span-wise oscillations are also present. These wave phenomena are ideally tracked by looking at how the different points of the measurement domain are shifted one about the other, and thus considering the coherence of the pressure fluctuations:

$$C_{xy}(f) = \frac{|P_{xy}(f)|^2}{|P_{xx}(f)||P_{yy}(f)|}$$

where $x$ is taken at all the locations of the PSP plane and $y$ serves as a reference point for phase and amplitude. The spectral power density $|P_{ab}|$ of two signals $a$ and $b$ is here evaluated using Welch method, with segments of data of 1024 samples, overlap of 50%, resulting in averaging over 20 segments. Figure 12 shows the coherence maps of the pressure fluctuations when buffet is present, for the turbulent and laminar cases. Coherence maps indicate that the turbulent phenomenon is well correlated with the entire flow field, at least the part that is captured by the PSP domain. In the laminar case, the correlation is limited to the region of the shock wave, upstream of it and downstream with a limitation in span. This shows that the laminar phenomenon does not imply a global oscillation as in the turbulent case but rather govern the flow dynamics over the downstream second half, in chord, of the airfoil.

The curves show the span-wise averaging time shift of the pressure data. Note that span-wise average allows removing the noise otherwise present in each individual chord line. A linear fit of the data for segments of these curves yield the phase velocity of the propagation phenomena. In the turbulent case, the phase velocity agrees with the value given by Jacquin et al. [**2**]. In the laminar case the propagation occurs in two opposite directions, upstream ahead of the shock (at a velocity equal to $-48.4m/s$) and downstream in the region under the shock and behind it, with an acceleration of the phase speed from about $18m/s$ to approximately $45.5m/s$ at approximately 58% of chord. The dip in the curve in Figure 12b at this position is associated with the shock wave that lies there.

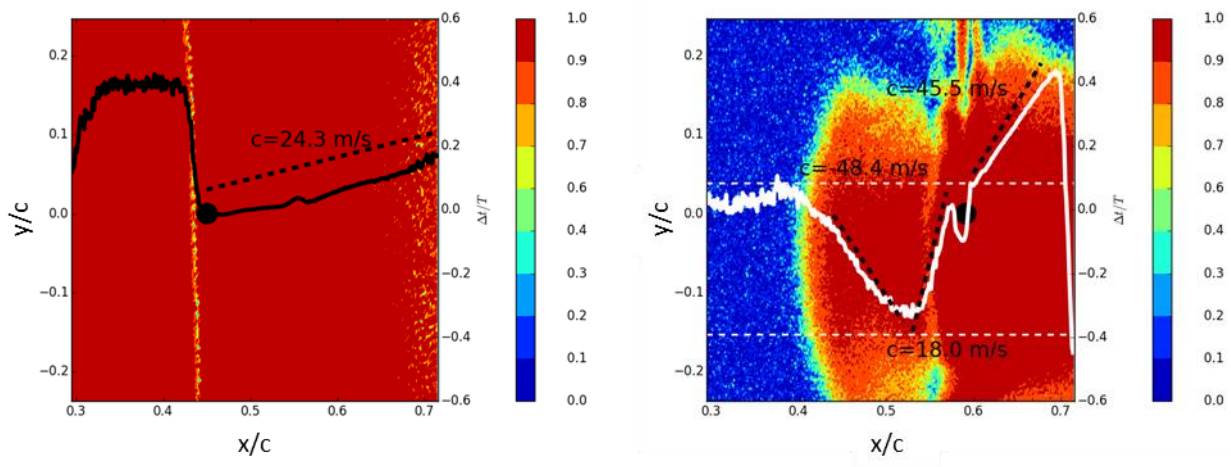


a) Turbulent f=72Hz b) Laminar f=883Hz

**Figure 12. Maps of coherence of the pressure field at M=0.735 for (a) the turbulent and (b) laminar modes. Colored iso-contours show the coherence of the pressure fluctuations over the measurement domain and the curves show a span wise average of the time shift (normalized on the period *T* associated with the selected frequency) between the measurement and reference points (indicated by the large black dot). In the laminar case (a), the span wise averaging is limited to the zone in between the dashed lines. Linear fits of the different parts of these curves allow calculating the phase velocity of the waves.**

## IV. Conclusion

An experimental analysis of the shock dynamics on a laminar airfoil in the transonic regime has been performed using an unsteady PSP coating to capture the pressure fluctuations at the upper surface. The goals of these tests were to validate the capability of the unsteady PSP to assess the unsteadiness of the flow over the laminar airfoil in buffet conditions.

It is demonstrated that the surface roughness of anodized-aluminum PSP is adequate for the laminar flow conditions. In general this should be considered as an issue for PSP coatings, as well as the way PSP is implemented in the model. The anodized-aluminum PSP used here requires an insert which has been suspected to affect the pressure distributions at the edge of the insert, due to misalignment problems with the rest of the model. The problems of illumination and of model displacement have been identified and should be tackled in future work to improve the PSP technique.

The laminar shock dynamics could be fully retrieved by the PSP technique, with a peak at about 883Hz and the first harmonic at twice this frequency. Spectral analysis revealed a chord-wise extent of about 20% of chord and a large pattern of energy toward the trailing edge. In the turbulent case, the fluctuations of the shock wave under buffet condition have an extent of about 9% of chord. The dominant mode is at 72Hz with the presence of several harmonics. The PSP images also clearly bring out a weaker second shock, downstream of the main one. Moreover, span wise fluctuations of the flow field are observed, traducing span-wise deformations of the shock wave. Coherence maps have been used to identify the correlation of pressure fluctuations over the PSP insert and retrieve the phase velocity of the propagation phenomena.

## References

[1] Lee, B. H. K., "Self-sustained shock oscillation on airfoils at transonic speeds," *Progress in Aerospace Sciences*, vol. 37, no. 2, pp. 147-196, 2001.

[2] Jacquin, L., Molton, P., Deck, S., Maury, B., Soulevant, D., "Experimental study of shock oscillation over a transonic supercritical profile," *AIAA Journal*, vol. 47, no. 9, pp. 1985-1994, 2009.

[3] Dandois, J., "Experimental study of transonic buffet phenomenon on a 3D swept wing," *Physics of Fluids*, vol. 8, no. 1, 2016.

[4] Dor., J. B., Mignosi, A., Seraudie, A., Benoit, B., "Wind tunnel studies of natural shock wave separation

instabilities for transonic airfoil tests," in *Symposium Transonicum III, Springer*, 1989, pp. 417-427.

[5] Brion, V., Dandois, J., Abart, J.C., Paillart, P., "Experimental Analysis of the Shock Dynamics on a Transonic Laminar Airfoil," *Progress in Flight Physics*, vol. 9, pp. 365-386, 2017.

[6] Gregory, J.W., Sakaue,H., Liu,T., Sullivan,J.P., "Fast pressure-sensitive paint for flow and acoustic diagnostics," *Annual Review of Fluids Mechanics*, vol. 46, 2014.

[7] Asai, K., Amao, Y., Iijima, Y., Okuda, I., Nishide, H., "Novel Pressure-Sensitive Paint for Cryogenic and Unsteady Wind Tunnel Testing," in *Aerospace Sciences Meeting and Exhibit*, AIAA 2000-2527.

[8] Sakaue, H., Gregory, J.W., Sullivan, J.P., Raghu, S., "Porous Pressure-Sensitive Paint for Chararacterizing Unsteady Flowfields," *AIAA Journal*, vol. 40, no. 6, 2002.

[9] Sakaue, H., Tabei, Y., Kameda, M., "Hydrophobic Monolayer Coating on Anodized-Aluminum Pressure-Sensitive Paint," *Sensors and Actuators B*, vol. 119, 2006.

[10] Mérienne, M.-C., Le Sant, Y., Lebrun, F., Deléglise, B., Sonnet, D., "Transonic Buffeting Investigation using Unsteady Pressure-Sensitive paint in a Large Wind Tunnel," in *51st AIAA Aerospace Sciences Meeting*, Grapevine, USA, AIAA 2013-1136.

[11] Sugioka, Y., Numata, D., Asai, K., Nakakita, K., Koike, S., Koga, S., "Unsteady PSP Measurement of Transonic Buffet on a Wing," in *53rd Aerospace Sciences Meeting*, AIAA 2016-0025.

[12] Brion, V., Reijasse, P., Dandois, J., Abart, J. C., Paillart, P., "Laminar buffet and flow control," in *EUCASS Conference*, Milan, Italy, 2017.

[13] Le Sant, Y., Deléglise, B., Mébarki, Y., "An Automatic Image Alignment Method Applied to Pressure-Sensitive Paint Measurements," in *ICIASF'97*, Monterey, 1997.

[14] Michou, Y., Deléglise, B., Lebrun, F., Scolan, E., Grivel, A. Steiger, R., Pugin, R., Mérienne, M.C., Le Sant, Y., "Development of a Sol-Gel Based Nanoporous Unsteady Pressure-Sensitive Paint and Validation in a Large Transonic ONERAS's S2MA Wind Tunnel," in *31st AIAA Aerodynamic Measurement Technology and Ground Testing Conference*, AIAA 2015-2408.